Intrinsic Segmental Flexibility of the S-1 Moiety of Myosin Using Single-Headed Myosin†

Robert Mendelson* and Pearl Hung-Chu Cheung

ABSTRACT: The fluorescence depolarization of *N*-iodoacetylamino-1-naphthylamine-1-sulfonic acid (1,5-IAEDANS) labeled myosin and single-headed myosin has been measured in order to study the intrinsic flexibility of the S-1 moieties and the mechanical interaction between the moieties. Data for soluble protein showed only a small decrease in rotational relaxation time when one head was removed. Single-headed myosin synthetic filaments gave the long decay time that has been found for similar myosin synthetic filaments. Results on soluble proteins verify the notion of a localized highly flexible region between S-1 and S-2. These results also fit hydrodynamic predictions based on a model in which S-1 moieties pivot independently (with some possible steric hindrance) about the S-1–S-2 junction. Adding different nucleotides, nucleotide analogues, and calcium ions to heavy meromyosin (HMM) and filaments showed no evidence for changes in flexibility, shape, or radial movement of crossbridges. Removal of Nbs_2 light chain did not eliminate immobilization upon forming thick filaments: thus, they do not appear to have a role in binding crossbridges to the thick filament during relaxation. Numerical calculations of fluorescence depolarization of dipoles diffusing within cone-shaped boundaries have been performed. These calculations showed that the immobilization seen in synthetic and native thick filaments is consistent with the S-1 moieties moving within a cone of half angle of less than 12.5° in relaxed muscle.

Flexibility within muscle crossbridges has been postulated from electron microscopy (Reedy et al., 1965; Huxley, 1969), X-ray diffraction (Huxley & Brown, 1967; Miller & Tregear, 1972), and mechanical studies (Huxley & Simmons, 1971) to allow for rotational motion of myosin heads during contraction. The enzymatic degradation of myosin (Lowey et al., 1969) has indicated that a highly susceptible site exists between the globular S-1's[1] and the rod portion, and thus it should be a good choice for a flexible region. In a previous work, Mendelson et al. (1973) studied this question by measuring the fluorescence depolarization of specifically labeled myosin heads undergoing rotational Brownian movement. The rates of decay of fluorescence polarization anisotropy from S-1, heavy meromyosin (HMM), and myosin indicated an elongated S-1 moiety which tumbled as if connected by a "universal joint" between S-1 and the rods (if the presence of the other head were ignored). Further, it was found that when myosin was assembled to form synthetic filaments, or was in myofibrils, this rotary mobility was greatly decreased. It was assumed that the ordering of the heads in the thick filament lattice, as seen in the highly developed layer lines of X-ray diffraction, gave rise to this immobilization. Mendelson and Cheung (1976) used this property to search for the effects of Ca^{2+} on the radial movement of S-1 moieties in synthetic thick filaments. The flexibility and immobilization results have been confirmed by Thomas et al. (1975a,b) using saturation transfer electron-spin resonance spectroscopy.

The recent isolation of one-headed myosin from papain digests (Margossian & Lowey, 1973a; Lowey & Margossian, 1974) suggested that these and other questions could be studied more directly. By comparing the fluorescence depolarization of one- vs. two-headed myosin, a measure of the mechanical interaction between the heads could be obtained. Additionally, single-headed myosin allows the study of the intrinsic mobility of the head, both in free myosin and within the aggregated filament, without possible interference by the other hand.

The data presented here show that both soluble and aggregated single- and double-headed myosin behave similarly. Results obtained with soluble myosin indicate that the heads are not mechanically linked and that the flexible region between S-1 and S-2 is not long. In the Appendix a numerical study of the theory of fluorescence depolarization with boundary conditions is presented. This theory is used to estimate the range of angular movement of heads in synthetic filaments. In the model considered it is found that this range is less than $\pi/3$ steradians, indicating that rotation of the heads is probably mechanically hindered by the filament lattice.

Materials and Methods

Preparation of Labeled Myosin and Myosin Fragments. A solution, used for labeling myosin, was made by dissolving *N*-(iodacetylamino)-1-naphthylamine-5-sulfonic acid (1,5-IAEDANS) (Aldrich Chemicals) in 0.5 M Tes, pH 7, buffer to a concentration of 1.7 mg/mL. Because the dye was photolabile, its viability was occasionally examined on paper chromatography.

Myosin, prepared by the method of Tonomura et al. (1966), was labeled in 0.6 M KCl at pH 7 with 1.0–1.33 mol of dye/mol of myosin. The labeling solution was stirred into the myosin, and, after a 24-h period, the mixture was dialyzed against dye-free buffer to remove reaction products.

HMM and S-1 were prepared with digestion conditions and chromatography as described previously (Mendelson et al., 1973). In one preparation of HMM, 1 mM $MgCl_2$ was added before digestion to increase the amount of Nbs_2 light chain retained (Margossian et al., 1975). S-1 proteolysis by trace

† From the Cardiovascular Research Institute, University of California, San Francisco, California 94143. *Received October 18, 1977.* This work was supported by United States Public Health Service Program Project Grants HL-06285 and HL-16683 and National Science Foundation Grant PCM-76-11491.

[1] Abbreviations used: DTT, dithiothreitol; EGTA, ethylene glycol bis(β-aminoethyl ether)-*N,N'*-tetraacetic acid; 1,5-IAEDANS, *N*-iodoacetylamino-1-naphthylamine-1-sulfonic acid; Tes, *N*-tris[hydroxymethyl]methyl-2-aminoethanesulfonic acid; TLCK, 1-chloro-3-tosylamido-7-amino-L-2-heptanone hydrochloride; Tris, tris(hydroxymethyl)-aminomethane. Myosin fragments: Nbs_2 light chain, the light chain removed by treatment with 5,5'-dithiobis(2-nitrobenzoic acid); HMM, heavy meromyosin; S-1, subfragment 1; S-2, subfragment 2.

0006-2960/78/0417-2139$01.00/0

papain was eliminated by adding 5 μM TLCK to the final buffer. When preparing HMM, 1 mM DTT was added to the tryptic digest to eliminate oxidation that would otherwise occur during the relatively long chromatography time (see Mendelson et al., 1975).

Preparation of Labeled Single-Headed Myosin. In order to prepare large amounts of single-headed myosin rapidly, we have modified the purification technique of Margossian & Lowey (1973a). The method reported here is based on the large difference of affinity of S-1 and HMM for actin (Margossian & Lowey, 1973b, 1976; Highsmith, 1977). It was found that this difference of affinity ($K_{HMM} > 10K_{S\text{-}1}$) also applies to single-headed myosin and myosin. Low salt conditions, where actin affinity was highest, were used to precipitate both actomyosin and single-headed actomyosin and thereby purify against papain and rod. High salt and low actin concentrations were used to produce conditions favorable to the selective precipitation of actomyosin from a mixture of actin, myosin, and single-headed myosin.

Labeled myosin (15 mg/mL) was dialyzed against 0.2 M ammonium acetate at pH 7.2 and then digested by soluble papain ($1\text{-}3 \times 10^{-2}$ mg/mL) for 15 min at 25 °C (Lowey & Margossian, 1974). The papain (1.0 mg/mL) stock solution, containing 5 mM EDTA, 0.2 mM DTT, 40 mM KCl at pH 7, was diluted 30- to 100-fold into precipitated myosin. Because of variability in proteolysis, the amount of papain required was determined by making a trial digestion of 100 mg of myosin. By stopping the reaction (described below) and measuring the optical density of the soluble products the approximate S-1 yield was obtained. The concentration of papain was then readjusted to give an S-1 yield of about 50%. This yield was selected because it gave, assuming equal probability of digestion of both myosin heads, the maximal absolute single-headed yield, which was twice as large as both myosin and rod.

The papain digestion was stopped in the following manner. A sixfold volume dilution in cold 20 mM Tes, pH 6.5, buffer was followed by centrifugation for 3 min at 80 000g. The pellet was then washed and homogenized (using a Teflon homogenizer) in 4 volumes of 20 mM Tes, 30 mM KCl (pH 6.5) and centrifuged for 10–15 min at 80 000g. This process was repeated twice with final suspension and homogenization in 0.22 M KCl, 10 mM Tris, and 1 mM $MgCl_2$, pH 8 (0 °C). The first fraction, enriched in papain-exposed myosin, was then obtained by adding 0.1 mol of actin/mol of single headed myosin (computed from absorbance and assumed relative yields), centrifugation for 15 min at 80 000g, and collecting the pellet. Subsequent centrifugation of the pellet material in high salt buffer with 0.1 mM magnesium pyrophosphate for 1.5 h at 140 000g removed the actin. The second fraction, purified to eliminate myosin, was obtained by first adding 100 mg of actin to the supernatant, centrifugation for 10 min at 80 000g, homogenizing the pellet, and repeating the centrifugation. The pellet was then homogenized and diluted about fivefold so that the final buffer contained 0.5 M KCl, 50 mM KH_2PO_4/K_2HPO_4 at pH 7.0. This was then centrifuged for 1.5 h at 140 000g and the supernatant retained. A final purification to eliminate myosin further was accomplished by adding 0.15 mol of actin/mol of single-headed myosin (computed from absorbance assuming no contribution from rod or myosin) and again centrifuging at 140 000g for 1.5 h. A few micromoles of TLCK was added to single-headed myosin to inhibit further proteolysis by trace papain.

Although S-1 could not be detected on either nondenaturing or $NaDodSO_4$ gels, as a precautionary measure, immediately prior to data collection, any newly generated S-1 was removed by dialysis against low salt and centrifugation.

The pellet was resuspended in 0.5 M KCl, 0.1 mM magnesium pyrophosphate, 50 mM phosphate buffer at pH 7, and single-headed myosin and control myosin were spun for 1.5 h at 140 000g to eliminate large aggregates.

This method of preparation produced 30 to 50 mg of single-headed myosin (see Results) from 1 g of myosin. The preparation time was about 24 h.

Preparation of Rod. Rod was prepared from labeled myosin by digestion under the same conditions as those used for single-headed myosin, except that the digestion time was 30 min. The reaction was stopped by dilution in cold 20 mM Tes, 30 mM KCl, 1 mM iodoacetic acid at pH 6.5 and subsequent centrifugation. The pellet was resuspended in high salt (5–10 mg/mL), and globular proteins were denatured by slowly adding 3 volumes of ice-cold ethanol (Szent-Györgyi et al., 1960) to the stirring protein solution.

This solution was then centrifuged at 80 000g, and the resulting pellet was washed, homogenized, and exhaustively dialyzed against 0.5 M KCl, 50 mM phosphate buffer at pH 7. Centrifugation at 80 000g for 20 min removed denatured proteins. A final purification and concentration increase were effected by dialysis of the supernatant against 20 mM Tes, 30 mM KCl, pH 6.5, centrifugation, and resuspension in 0.5 M KCl, 50 mM phosphate buffer at pH 7.

Preparation of 1,5-IAEDANS Myosin Depleted in Nbs_2 Light Chain. 1,5-IAEDANS-labeled myosin was treated with Nbs_2 and EDTA using the method described by Weeds & Lowey (1971). Prior to fluorescence depolarization experiments the sample was spun at 140 000g for 3 h to remove any aggregates.

Characterization of Proteins and Fluorescence Measurements. Proteins were examined for purity on 5 and 10% acrylamide gels containing sodium dodecyl sulfate ($NaDodSO_4$) and on 3% acrylamide nondenaturing gels. The nondenaturing gels contained 20 mM $NaPP_i$ and 1 mM $MgCl_2$ in Tris–glycine buffer. The samples were dissolved in a solution containing 50% glycerol, 2 mM $NaPP_i$, and 0.1 mM $MgCl_2$ and electrophoresed at 20 mA for 12–14 h at 4 °C.

Sedimentation studies were made on a Beckman Spinco analytical centrifuge.

Electron microscopy studies of synthetic thick filaments were made using 1% uranyl acetate negative staining on carbon-coated grids. Micrographs were made using a Phillips 201 electron microscope.

Ca^{2+}-ATPases were measured at pH 8 by determining the liberated P_i. Protein concentrations were measured using extinction coefficients $E_{280nm}^{1\%}$ of 5.43 cm^{-1} for myosin, 7.8 cm^{-1} for S-1, 2.85 cm^{-1} for myosin rod, and 4.6 cm^{-1} for single-headed myosin; the molecular weights used were, respectively, 450 000, 115 000, 220 000, and 335 000. The extinction coefficients and molecular weights for rod and single-headed myosin were calculated from the S1 and myosin data of Lowey et al. (1969).

Fluorescence depolarization measurements were made using a nanosecond-decay fluorimeter optimized for these studies (Mendelson et al., 1975). Excitation light was produced by a spark-gap in air and monochromated by Corning 7-60 and 0-52 glass filters which gave a mean excitation wavelength of 375 nm. Emission light was selected by a Corning 0-51 glass filter and by two specially made Corion Corp. (serial no. 644980) filters which passed light of wavelength greater than 450 nm. Quinine sulfate calibrations allowed small corrections to be made for zero-time differences and overall quantum efficiency differences between the two (polarized) intensity branches of the instrument. The solution temperature was 5 °C in all experiments.

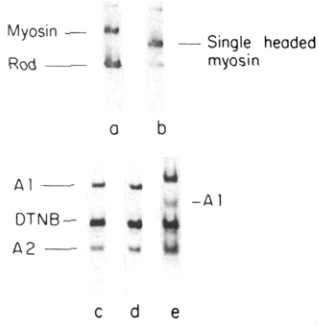

FIGURE 1: (a) Nondenaturing gels of a mixture of equal weights of myosin and rod (a) demonstrating the heavier staining of rod and of a single-headed myosin preparation (b) run concurrently with gel (a). $NaDodSO_4$ (10% polyacrylamide) gels of myosin (c), 1,5-IAEDANS-labeled myosin (d), and 1,5-IAEDANS-labeled single-headed myosin light chains (e). For $NaDodSO_4$ gels, proteins were precipitated with 10% trichloroacetic acid and washed with ethanol and ether.

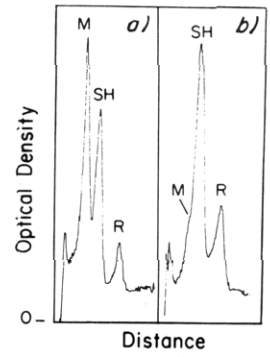

FIGURE 2: Photograph of densitometer scan of nondenaturing native gels of (a) the papain-exposed myosin-rich fraction and (b) the single-headed myosin preparation.

Rotational relaxation times (ϕ) were determined by an exhaustive search procedure which determined the best fitting single exponential function within a chosen time interval. The criterion for the best fit was that the weighted chi-squared function be at a global minimum. The weighting function for chi-squared was calculated by assuming the polarized intensities photon fluxes each obeyed Poisson statistics. The fitting interval was chosen to be between 26 and 113 ns after the peak polarization. This interval minimized contributions from initial (light scatter and electronic) transients, from effects of aggregates, and of the finite time response instrument. The effect of finite time response was investigated by convoluting the system response to scattered light with intensity expressions for equivalent spherical molecules (Yguerabide, 1972).

In measurements where turbidity was significant, a depolarization occurred because the excitation geometry was altered; this alteration caused emission light rays to be moved in space and in some cases miss the photomultiplier entirely. This effect was corrected for by iteratively altering the peak polarization to that expected for a particular rotational correlation time. The expected peak polarizations were determined by using varying amounts of HMM and actin or HMM in varying amounts of glycerol.

Steady-state fluorescence measurements were made using a Perkin-Elmer MPF-4 fluorimeter.

Results

Characterization of 1,5-IAEDANS-Labeled Single-Headed Myosin. The purity of the single-headed myosin preparation was routinely monitored using nondenaturing (3%) polyacrylamide gels with Coomassie blue staining. These gels were calibrated for protein peak position, relative staining of the different proteins, and linearity with varying amounts of protein by making companion gels with differing amounts of rod and myosin or a rod–myosin mixture (Figure 1).

Since single-headed myosin is a mixture of the heavy chain of both rod and myosin, it was assumed that its relative staining intensity would be obtained by interpolation between those of myosin and rod. Densitometry of the gels showed that for an equal weight of myosin and rod the rod stained 2.2 times as heavily; hence, the single-headed myosin was assumed to be stained 1.6 times as heavily as myosin. Thus, for gels containing an equal number of moles of myosin, single-headed myosin, and rod, the areas of the peaks would be in the ratio of 1.0:1.2:1.1. Analytical ultracentrifuge studies of several single-headed myosin preparations gave essentially one peak in Schlieren pattern. The sedimentation constant of this peak (one preparation) was intermediate between that of myosin and rod, thus verifying the gel patterns. The optical density of gel staining was found to be linear over the region of protein concentrations used for myosin and rod. Densitometry of single-headed myosin gels (Figure 2) showed that typically the corrected molar ratio of myosin–single-headed myosin–rod equaled <0.03:1.0:0.25. This ratio was quite reproducible, though preparations could be further purified against myosin at the expense of increasing the relative amount of rod. Actin contamination in single-headed myosin preparations was estimated from $NaDodSO_4$ gels to be less than 2% of the single-headed myosin. $NaDodSO_4$ gels of rod showed a single peak containing greater than 95% of the protein.

The $NaDodSO_4$ gel patterns of labeled single-headed myosin heavy chain were similar to those of S-1 added to rod heavy chain, in agreement with the Lowey & Margossian (1974) preparation. $NaDodSO_4$ gels in the heavy-chain region showed the expected myosin heavy chain, a chain of slightly lower molecular weight with a lower yield and a chain with the molecular weight of rod heavy chain. The light-chain region (Figure 1) showed a heavy-chain fragment, a degraded Al, and virtually intact Nbs_2 and A2 light chains. Densitometry showed the Nbs_2 and A2 light chains were present in approximately the same molar ratios, to complete single-headed myosin heavy chains, as the light chains in intact myosin were to myosin heavy chain. The ratios of A2 to Nbs_2 peak areas could be more accurately measured and were found to be the same as in myosin, within approximately 25%. Because of degradation the only conclusion that can be drawn is that Al is present at least 50% as much as in myosin. Thus, if A1 were approximately uniformly distributed in the mass of the S-1 moiety in native myosin, about a 10% decrease in ϕ value might be found for single-headed myosin due to a mass deficit alone. Since there is some extra material in the Nbs_2 and A2 light-chain region, it is likely that much less than 50% of the A1 light-chain peptides were actually removed from the single-headed myosin.

The molar Ca^+-ATPase of labeled single-headed myosin ranged from 70 to 90% of half of that of the control myosin sample (which had been exposed to the same proteolysis buffer and temperature). The labeling conditions used here (0.66 dyes/myosin head) produced an activation of about fourfold, in agreement with earlier work (Mendelson et al., 1975; Takashi et al., 1976) in which a six- to sevenfold activation was found for fully modified myosin.

The activation and the peptide mapping (Takashi et al., 1976) provide evidence of highly specific labeling of a single fast-reacting thiol on each head of myosin. To quantify the specificity of labeling further, the fluorescence per mole (F)

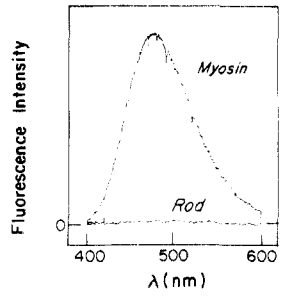

FIGURE 3: Photographs of scans of (uncorrected) fluorescence emission spectra of 1,5-IAEDANS-labeled myosin and of rod generated from this myosin. The molar concentrations of rod and myosin were approximately equal.

of the labeled myosin was compared with that of rod (Figure 3) and with that of single-headed myosin, both of which were separately generated from the labeled myosin. The results, corrected for rod contamination, were:

$$\frac{F(\text{myosin})}{F(\text{rod})} \simeq 120$$

and

$$\frac{F(\text{myosin})}{F(\text{single headed myosin})} = 2.22 \pm 0.20$$

(SEM for $n = 5$).

Fluorescence Depolarization of Single-Headed Myosin under High Salt Conditions. Figure 4 shows a comparison of fluorescence depolarization curves from a myosin control, a papain-exposed fraction enriched in myosin (see Materials and Methods), and single-headed myosin, all in high KCl. The densitometer tracings of nondenaturing gels of these fractions are shown in Figure 2. In order to obtain the effective molar contribution to fluorescence depolarization data, the area of the myosin peak in these gels must be multiplied by 1.2 for differences in molecular weight and Coomassie staining and additionally by 2 to correct for quantum yield. Thus, the myosin-enriched data contained about a 75% myosin contribution. As can be seen in Figure 4 and Table I, there is no significant difference between the data from the myosin-enriched fraction which had been exposed to papain and that data from the myosin control which had been dialyzed against the ammonium acetate proteolysis buffer but had not been exposed to papain. Preparations which were identical as far as light-chain composition and ATPase and myosin impurity are included in the average in Table I.

Two potential sources of error in these experiments were differences in reversible intramolecular or intermolecular interactions and differences in denaturation and subsequent aggregation. The concentration dependence (0–4 μM) of polarization decay was found to be negligible ($|\text{slope}| < 5$ ns/μM), indicating that reversible association had a negligible effect under these ionic conditions. Recently, Margossian & Lowey (1977) reported a reversible calcium-dependent self-association of S-1 fragments. The fluorescence depolarizations of myosin and single-headed myosin used here were found to be identical within statistical error when either 1 mM EGTA (pCA $\simeq$ 8.5) or 0.1 mM $CaCl_2$ (pCa $\simeq$ 4) was added, so that this effect was not significant in our experiments. Thus, we conclude that reversible intermolecular and intramolecular interaction did not introduce significant error in these experiments.

Effects due to denaturation and subsequent aggregation were discernible, however. In one experiment, single-headed myosin was made from freshly prepared myosin, and the depolarizations were found to be quite similar. One month later, single-headed myosin was made from the same myosin that had been glycerinated; the decay time of myosin had significantly increased, but the single-headed myosin retained approximately the same absolute value. Other measurements

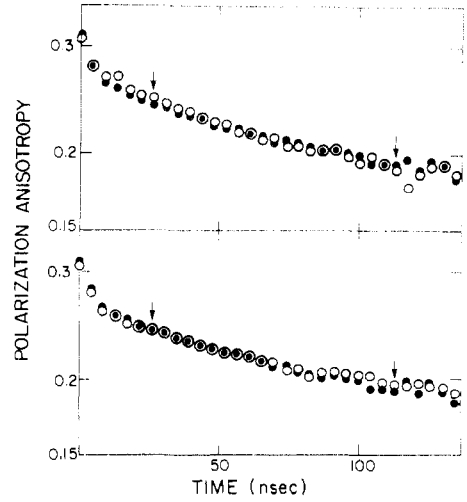

FIGURE 4: Fluorescence depolarization of preparations shown in the densitometer scans in Figure 2. The top curves are for single-headed myosin (●) and the papain-exposed myosin fraction (○). The bottom curves are of the same single-headed myosin (●) and its parent myosin (○). All proteins were in 0.5 M KCl, 0.1 mM magnesium pyrophosphate, 50 mM phosphate buffer at pH 7. Arrows indicate the limits of the time region used to determine the rotational relaxation time (ϕ).

TABLE I: The Fluorescence Depolarization of Single-Headed Myosin in Different Media.

Initial system	Final system	$100 \times (\Delta\phi/\phi)$ (%)[e]	No. of preps
Soluble myosin[a]	Soluble single-headed myosin[a]	−9 ± 1.8	6
Soluble myosin[a] (papain-exposed)[d]	Soluble myosin[a]	+3 ± 2	4
Soluble single-headed myosin[a]	Single-headed myosin filaments[b] (pH 6.3)	+530 ± 70	3
Soluble myosin[a]	Myosin filaments[b] (pH 6.3)	+460 ± 60	3
Soluble single-headed myosin[a]	Single-headed myosin filaments (pH 8.0)[c]	+200	1
Nbs_2-treated soluble myosin:	Nbs_2-treated myosin filaments:		
pCa 4	pCa 4	+400	2
pCa 8.5	pCa 8.5	+350	2
Single-headed myosin filaments (pH 6.3)	Single-headed myosin filaments + tenfold excess of F-actin	+200	1

[a] 0.5 M KCl, 0.1 mM magnesium pyrophosphate, 50 mM phosphate buffer (pH 7). [b] 0.1 M KCl, 0.1 mM magnesium pyrophosphate, 50 mM phosphate buffer (pH 6.3). [c] 0.1 M KCl, 0.1 mM magnesium pyrophosphate, 0.05 M Tris-HCl (pH 8). [d] This myosin was exposed to papain under the same conditions as was the single-headed myosin. About 75–80% of the fluorescence in these samples arose from myosin and 20–25% arose from single-headed myosin (see text and Figure 2). [e] Values given are means and standard errors of the mean.

with 2 to 3 week old myosin and single-headed myosin gave similar results. This suggested that irreversible aggregation of myosin could have been occurring more rapidly. For this reason, all experiments were done as soon after preparation as possible, usually within 36 h after papain digestion. Some aggregation was always present, however, even immediately after high-speed centrifugation. Schlieren patterns and densitometry of native gels showed that aggregates amounted to at most 5% of the total protein and that the difference in amount of aggregation between single-headed myosin and myosin preparations (of equal molar concentration) was never more than ±3% of the total amount of each protein. Because the depolarization experiments were done within 1 h after high-speed centrifugation and the gels and analytical centrifuge were not run until 3 h to 2 days after centrifugation, the amount of aggregation seen was probably an upper limit to that present during the experiments. Numerical calculations estimated the upper limit on the expected change in ϕ value because of aggregates (assuming the ϕ value of aggregates to be infinite) at 3%; therefore, aggregation of all kinds was considered to have a negligible effect on these data.

If the rod portion of the myosin contained significant label, there would have been an artifact introduced into depolarization data by the rod depolarization which would have twice the contribution to single-headed myosin data as to myosin data. Fortunately, the labeling of the rod was weak (see above) and the decay time of rod alone was fast ($\phi < 400$ ns) so that its effect on the data, as shown by numerical studies, was negligible (<1%).

Another possible source of error is head-to-head energy transfer which would cause depolarization. Although this was unlikely because of the large difference between peak excitation wavelength (340 nm) and peak emission wavelength (480 nm), it could not be ruled out a priori. This was investigated by measuring the decay time (ϕ) as a function of moles of dye per moles of myosin in the labeling mixture. Since the purity of the dye was estimated to be greater than 90% and the incubation time was very long compared to the labeling time constant, it is assumed that this is equivalent to measuring the ϕ value as a function of dye bound. There was no discernible change in ϕ value with increasing dye concentration (0.2–2 mol of dye/HMM); hence, intramolecular energy transfer was negligible.

Measurements with added actin showed that even with equimolar actin and myosin the binding was immeasurably small in the presence of 0.1 mM magnesium pyrophosphate. Thus, actin contamination in the single-headed myosin preparation had a negligible effect on the data.

Fluorescence Depolarization of Single-Headed Myosin Synthetic Filaments. Myosin and single-headed myosin were dialyzed against the low KCl buffers used by Lowey & Margossian (1974). In agreement with their work, it was found that spindle-shaped synthetic filaments of similar length (~1.2 μM) were formed in a buffer containing 0.1 M KCl, 50 mM phosphate buffer at pH 6.3. Filaments of rod produced under the same conditions were found to be somewhat shorter (~0.9 μm).

The fluorescence depolarization of myosin and single-headed myosin filaments are shown in Figure 5. The (pH 6.3) single-headed myosin filaments show a slightly larger increase in decay time than myosin (at the same molar concentration) and both appear to have a biphasic decay curve which is probably indicative of a fraction of the molecules being less immobilized. Filaments dialyzed against the pH 8 buffer used by Margossian & Lowey (1974) exhibited much greater mobility, in agreement with similar observations on myosin filaments (Thomas et al., 1975b; Mendelson & Cheung, 1976).

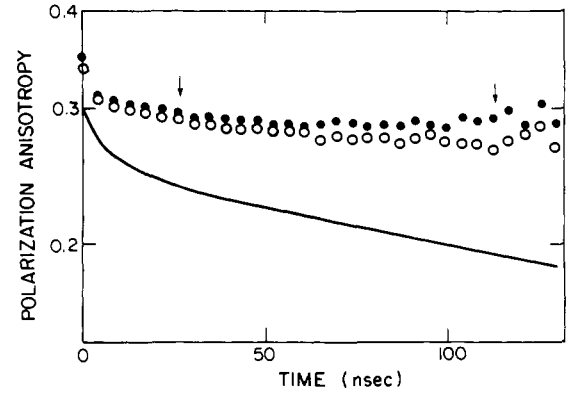

FIGURE 5: Polarization anisotropy decay of single-headed myosin (1.4 μM) (●) and myosin synthetic (1.4 μM) (○) filaments in 0.1 M KCl, 50 mM phosphate buffer at pH 6.3. The solid line is the polarization decay of soluble myosin.

To explore further the cause of this large immobilization, an experiment to measure the binding of (cleaved) S-1 fragments to filaments made of purified rod was performed. The fluorescence depolarization of S-1 (at the same molar concentration as used in single-headed myosin filament experiments) was measured in 0.1 M KCl, 0.05 M phosphate buffer at pH 6.3. Rod filaments, in the same buffer, were added to give a final equimolar concentration of rods and S-1. No significant increase in the ϕ value was observed ($100\Delta\phi/\phi <$ 10%). A control experiment in which HMM was studied in 0.5 M KCl, 50 mM phosphate buffer at pH 6.3 and also in 0.1 M KCl, 0.05 M phosphate buffer at pH 6.3 gave no difference in polarization decay showing that ionic conditions alone are not responsible for the immobilization.

The Nbs_2 light chain has been implicated with S-1 proteolysis (Biro, 1972; Bagshaw, 1976; Margossian et al., 1975) and indirectly with filament alteration (Morimoto & Harrington, 1974), suggesting that it might play some role in the S-1 moiety immobilization under low salt conditions. To study this possibility, the depolarization of Nbs_2-treated myosin in high and low salt conditions was measured. $NaDodSO_4$ gels of the preparation showed that about 60% of the Nbs_2 light chain was removed. Under high salt conditions, Nbs_2 myosin had a somewhat larger ϕ value than control myosin, which was probably caused by some intermolecular aggregation (clarification by centrifugation reduces ϕ); however, the large increase in ϕ value observed on going to low salt conditions was (with or without Ca^{2+} present) qualitatively the same as untreated myosin. Thus, the Nbs_2 light chain cannot be responsible for the immobilization.

Effects of Various Ligands on Polarization Decay. Previously, we have reported a search for the specific effects of Ca^{2+} on synthetic filaments (Mendelson & Cheung, 1976), MgATP on myosin in 0.6 M KCl, or of MgATP on S-1 length (l) (Mendelson et al., 1975). No macroscopic changes in either myosin or myosin filaments or S-1 ($\Delta l < 1$ nm) were found. Here we report a study of the specific effect of MgATP on HMM and myosin filaments under low salt conditions. The results, shown in Table II, show that there were no significant changes in the polarization decay times. Only in the case of MgATP binding to synthetic myosin filaments was there any effect; however, this change in ϕ value was probably due to a small decrease in pH caused by incomplete buffering of hydrolyzing MgATP. Thus, there was no observable change in S-1 macroscopic shape, HMM flexibility, or filament structure when these ligands were added.

TABLE II: Effect of Various Ligands on Myosin and HMM.

Initial system	Final system	100 ($\Delta\phi/\phi$) (%)[e]	No. of 15-min diff. trails
HMM[a]	HMM + MgATP[a]	0.8 ± 1.7	24
HMM[a]	HMM + MgADP[a]	3.6 ± 2.0	17
HMM[a]	HMM + MgAMPPNP[a]	−1.8 ± 2.4	10
HMM (pCa 8.5)[b]	HMM (pCa 4)[b]	0.6 ± 1.8	25
Soluble myosin[c] (pCa 8.5)	Soluble myosin[c] (pCa 4)	−0.2 ± 2.0	14
Synthetic[b] filaments (pCa 8.5)	Synthetic filaments[b] (pCa 8.5 + MgATP)	14 ± 5	36
Synthetic[b] filaments (pCa 4)	Synthetic filaments[b,d] (pCa 4 + MgATP)	8 ± 5	36

[a] These solutions contained 1 μM HMM in 50 mM Tes, 50 mM KCl, 1 mM DTT at pH 7 and a feeder system consisting of the following: 400 μM phosphoenolpyruvate, 0.04 μM pyruvate kinase, and 150 μM MgCl. Nucleotide or analogue concentration was 20 μM. Approximately one-third of the HMM was generated in the presence of 1 mM $MgCl_2$ to increase the retention of the Nbs_2 light chain. [b] These solutions contained 90 mM KCl, 40 mM imidazole, 0.3 mM $MgCl_2$, pH 6.8. 5 mM MgATP was used when appropriate. The Ca^{2+} concentration was set by adding either 1 mM EGTA or 0.1 mM $CaCl_2$. The same conditions were used by Morimoto & Harrington (1974) and Mendelson & Cheung (1976). [c] These solutions were the same as in footnote *b*, except that the KCl concentration was 0.6 M. [d] A search for a specific effect of Ca^{2+} on the radial movement of S-1 moieties under these ionic conditions was reported by Mendelson & Cheung (1976). [e] Values given are means and standard errors of the mean.

Discussion

In the work of Mendelson et al. (1973) it was found that the S-1 moieties appear to have considerable freedom of motion with respect to the myosin stem. This was based on two levels of reasoning. The first involved a comparison of the relative rotational correlation times of S-1 and myosin given the observation that the absorption and emission dipoles of the dye must be rigidly oriented near the major axis of the S-1 (which was assumed to have a shape resembling a prolate ellipsoid of revolution). This lead to the conclusion that considerable flexibility existed within HMM. The second level of reasoning was based on a quantitative comparison of the polarization decay times of S-1 and myosin using a model based on a hydrodynamic theorem derived by Yu & Stockmayer (1967). From this model it was argued that the S-1 moieties tumble as if attached by a flexible "universal" joint between S-1 and the rod. These arguments will be discussed in light of the present results.

The polarization decay time of single-headed myosin was found to be within 10% of that of myosin, thus confirming that the results from myosin and HMM data reflected the intrinsic motion of the S-1 moieties. The assertion that flexibility exists within HMM is further strengthened, however. Previously, it was argued that the observed depolarization could not come from dipoles aligned near right angles to the rod of a perfectly rigid myosin molecule; if this were so, a much longer decay time would have been found. However, the lack of detailed hydrodynamic calculations prevented ruling out the (unlikely) possibility that the depolarization could arise from dipoles rigidly fastened at a more oblique angle to the myosin rod. The present single-headed myosin results preclude the possibility of myosin being a rigid "Y"-shaped molecule, because the removal of one of the arms of the "Y" would be expected to have a large effect on rotary diffusion about the rod axis.

Other possible rigid myosin configurations are more difficult to eliminate unambiguously on the basis of relative decay times alone. For example, the situation in which both heads were shaped like hemispheres that would bind together to give a sphere might cause a decrease in frictional resistance. This decrease could be of just the right magnitude to give the appropriate decay times for S-1, single-headed myosin, and myosin. Evidence against this myosin configuration is found in the three-dimensional reconstruction of S-1 binding to actin (Moore et al., 1970); S-1 was found to be approximately symmetric about its long axis and each S-1 binds to an actin monomer as a separate entity. Further, electron micrographs of soluble myosin show two distinctly separated heads (Lowey et al., 1969), and in preparations of single-headed myosin it was found (using analytical centrifuge and native gels) that S-1 to single headed myosin affinity was very small.

The quantitative comparison of myosin data with hydrodynamic theory (Mendelson et al., 1973) supported the notion that S-1 moieties pivot independently and freely about the S-1–rod junction as if the steric hindrance caused by the other head and the rod did not exist. The present data, which showed only a slight increase in ϕ value when both heads were present, verified these assertions by indicating that this neglect was justifiable (at least for S-1). The reason for the similarity in ϕ values could be that each head was fastened to rod by a flexible chain of length comparable to S-1. However, this can be precluded because the ϕ value increases (about twofold) when S-1 is incorporated into single-headed myosin. Further, the increase in ϕ for single-headed myosin does agree with the Yu and Stockmayer theorem; also it would be difficult to imagine how the immobilization seen in thick filaments could occur if S-1 possessed such a high degree of rotational freedom.

A qualitative explanation for the lack of change in ϕ value with possible increased steric hindrance is found from the examination of the model of S-1 pivoting with a reflecting cone of half angle δ_{max} (see Appendix). In Figure 8 it is seen that unless the geometry is highly restricted (δ_{max} small) there is no significant effect on the ϕ value (measured over the fitting interval used here). A plausible model of an ellipsoidal S-1 moiety would have it moving freely within at least 2π steradians: in this case, almost no effect on ϕ would be expected. It should be noted that this model does not allow for the Brownian movement of the cone (the second head), so that the solid angle restriction in the model must be considered to be that from a time-averaged boundary; however, the very large increase seen only for a high degree of restriction is not expected to be altered by this limitation.

The results of this work are in accord with the recent work of Cooke & Franks (submitted for publication) who show that threads made of single-headed myosin and actin produce half the force of actomyosin threads and thus that each head probably can function independently in muscle. The finding that myosin and single-headed myosin depolarize almost identically and S-1 moieties act as if they pivot independently at the S-1–S-2 junction precludes models in which heads are coordinated by light chains reaching between the heads (except at the pivot point). Cooperative action of the heads, as suggested by some authors (e.g., Tokiwa & Morales, 1971), could still occur by other modes.

The observation that single-headed myosin is highly immobilized in synthetic thick filaments is in accord with similar observations obtained for synthetic myosin filaments (Mendelson et al., 1973) and relaxed glycerinated myofibrils (Mendelson & Cheung, 1976). The decay curves for both

myosin and single-headed myosin filaments are biphasic, which could arise from restricted angular movement of equivalent S-1 moieties in the thick filament lattice even though detailed fits to the model considered in the Appendix could not be found. A likely cause for the shape of the curves is that some S-1 moieties in the thick filament possess greater freedom due to imperfect lattice formation (cf. Kaminer and Bell, 1966; Mendelson and Cheung, 1976). In the myofibril work a biphasic curve was not seen in accord with the latter hypothesis. Free myosin contributions can be excluded because about 10–20 times as much actin was required to eliminate mobility as was required for HMM under similar ionic conditions. Thus, the observed ϕ value for single-headed myosin is likely to be only a lower limit to that which would be observed in an ideal single-headed myosin thick filament. However, this does not allow (Figure 8) the setting of an upper limit of 15° on the half angle of the cone within which the S-1 moves. If the data on myofibrils ($\phi \simeq 3000$ ns) is considered, the angle is reduced to less than 12.5°. (The observed ϕ value could have contributions from free myosin or partially denatured myosin so only an upper limit on the cone half angle may be stated.) Thus, the heads are probably restricted on the average to a small angular range in relaxed muscle. The angle restriction could arise from S-1 being held in the filament lattice by compliance within the rod, or the S-1 heads could simply bind to the thick filament. No direct evidence pointing to the latter possibility has been found here or by others (cf. Lowey et al., 1969).

Some motion of the distal ends of the heads is required to allow the observed number of crossbridge–actin links to be made; the mismatch of thick and thin filaments periodicities would otherwise prevent a significant amount of binding. An approximate estimate of the angle may be made by noting that the fraction of heads bound is less than or equal to the extent of longitudinal position variation of a crossbridge divided by the thin-filament site spacing (cf. Schreiner, 1973). If there are only geometric limitations, then the equality is true. Assuming that the S-1's can bind equally well at the different angles through which they wobble, the maximum (half cone) angle (δ_{max}) can be estimated. For 50% of the S-1's bound, a 14-nm long S-1 and 5 nm between binding sites, the computed δ_{max} is about 10°. Thus, it may contribute to the synthetic filament mobility and also to the small difference between rigor and relaxation ϕ values observed with glycerinated myofibrils (Mendelson & Cheung, 1976).

The present results suggest that the crossbridges are in a fairly definite orientation (usually taken normal to the thick-filament long axis) in the relaxed state and prior to binding to the actin in stimulated muscle (Huxley, 1969). Actin binding could occur by the simple Brownian movement of the S-1's to their binding sites as suggested by the data of some workers (Nihei et al., 1974; Mendelson & Cheung, 1976; Sutoh & Harrington, 1977) or by Ca^{2+}-stimulated movement (Haselgrove, 1975). If the translational Brownian movement were responsible it would occur in the 10^{-7} s or longer time scale, depending on the compliance within the rod, compliance of the LMM–S-2 junction, and the distance between the distal portion of S-1 and the actin binding site. Since the crossbridge cycling frequency is of the order of 10–100 Hz (Curtin et al., 1974), only a very small fraction of the crossbridges need be near their binding site at any instant in order that a significant fraction would have made the excursion on a physiological time scale. The actin binding would be facilitated by increased rotary motion of the S-1 moieties occurring upon radial translation. After the end of the power stroke, which was presumably accompanied by a change in declination of the crossbridge of actin (Huxley and Simmons, 1971), the S-1 moieties would be restored to their equilibrium position near the thick filament. In sliding muscle, they would then be positioned over a new, downstream, binding site (Nihei et al., 1974; Mendelson and Cheung, 1976).

Acknowledgments

The development of the single-headed myosin preparation was done in collaboration with Dr. Roger Cooke; his generous sharing of equipment and techniques were invaluable.

We thank Dr. Jacqueline Hartt for making the electron micrographs and for reading the manuscript. We are indebted to Dr. Roger Cooke, Dr. Steven Harvey, Dr. Deborah Stone, and Professor Manuel Morales for many helpful suggestions.

Appendix: Numerical Studies of Fluorescence Depolarization with Boundaries

Below is presented the technique used for numerically computing the fluorescence depolarization predications of a dipole which pivots at one of its ends around a point located at the vertex of a cone. The dipole tumbles within the cone-shaped boundary subject to the rotary Brownian movement of the body which carries the dipoles, here chosen to be a prolate ellipsoid of revolution. The method used is an extension of that devised by Harvey and Cheung (1972) for solving the unbounded problem.

These calculations have been performed for a "perfect" dipole (absorption and emission dipoles coincident) with the dipole lying along the major axis of the ellipsoid of revolution. These approximations are justified experimentally; we have found (Mendelson et al., 1973; main text) that myosin subfragment 1 may be approximated by such a body carrying absorption and emission dipoles which nearly straddle the major axis and are only about 25° apart. Further, the region of fit in the experiments in the main text minimizes any small amount of fast-decaying components which would arise from the sensing of rotations about the major axis (which would occur if the dipoles were more nearly parallel to the minor axis) (cf. Belford et al., 1972). These rotations would not be affected by a boundary of the type considered here, so the fast-decaying components should not be altered when the barrier is imposed. The most general case can be considered by only a minor extension of the geometry presented.

Technique of the Calculation. The calculations were performed by generating an appropriate distribution of N pseudomolecules (typically 2000) and then following the time course of the polarized intensities ($I_{\parallel}(t)$ and $I_{\perp}(t)$) generated by each pseudomolecule as it underwent rotational Brownian movement. The polarized intensities from each pseudomolecule were finally number averaged, and from these average intensities the polarization anisotropy was computed according to the definition:

$$r(t) \equiv \frac{\overline{I_{\parallel}(t)} - \overline{I_{\perp}(t)}}{\overline{I_{\parallel}(t)} + 2\overline{I_{\perp}(t)}} \tag{1}$$

This number averaging over pseudomolecules is equivalent to averaging over N (random walk) trajectories, each one of which represents the trajectory of a set of a very large number of real molecules which are identically prepared.

A collection of randomly oriented classical dipoles, each having direction $\hat{\mu}$, is illuminated by a short burst of polarized radiation at time $t = 0$, as is shown in Figure 6. Prior to excitation, the dipoles fill space uniformly so that the number between the polar angle $\theta(0)$ and $\theta(0) + d\theta(0)$ is proportional to $\sin\theta(0)$ and the number between the azimuthial angle $\phi(0)$ and $\phi(0) + d\phi(0)$ is uniform. Hence, the number of dipoles excited

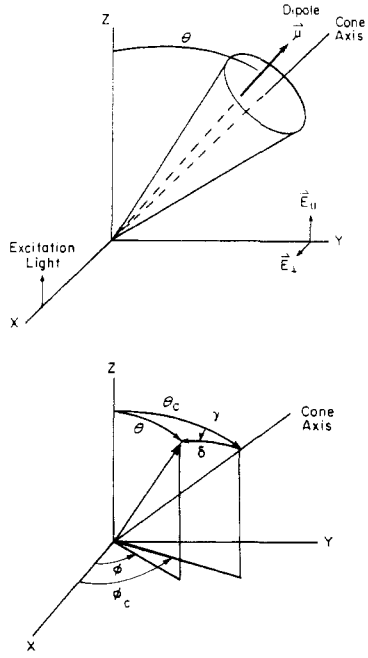

FIGURE 6: Top: The geometry of a fluorescence depolarization with the dipole diffusing within a cone shaped boundary. A single (macromolecular) cone and dipole are shown. Bottom: The detailed coordinate system used to generate rotations numerically and compute polarizations of dipoles diffusing within cone-shaped boundaries.

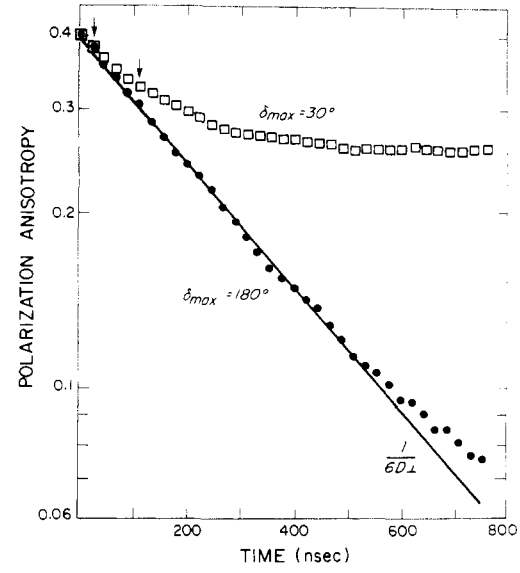

FIGURE 7: Numerically computed fluorescence depolarization curves for an S-1 moiety freely diffusing within a cone of half angle δ_{max}. The axial ratio of S-1 was taken to be 3.0, the partial specific volume 0.73 mL g^{-1}, the hydration 0.2 mL g^{-1}, T = 278 K, and the molecular weight 115 000. The arrows indicate the region used to determine the rotational and relaxation time (ϕ) throughout this work. The solid line is the theoretical unconstrained (δ_{max} = 180°) polarization anisotropy decay using the treatment of Belford et al. (1972) with the hydrodynamic theorem of Yu and Stockmayer (1965) (see text). 10^4 pseudomolecules were used in these computations.

at $t = 0$ will be proportional to sin $\theta(0)$ and also to the probability of excitation which is proportional to $\cos^2\theta(0)$. Also, the cones within which the dipoles lie are distributed proportional to sin $\theta_c(0)$, where θ_c is the polar angle of the cone axis, and uniformly around the azimuth $[\phi_c(0)]$.

In practice, the problem was simulated by first generating a set of cones with appropriately weighted coordinates, $[\theta_c(0), \phi_c(0)]$. Within each cone the dipole coordinates $[\delta(0), \gamma(0)]$ were chosen with a sine weight on $\delta(0)$ and a uniform weight on $\gamma(0)$ (see Figure 6). This procedure filled space uniformly with both cones and dipoles, thereby simulating the preexcitation condition. From these coordinates the initial coordinates of each dipole $[\theta(0), \phi(0)]$ were computed. The $\cos^2\theta(0)$ weighting factor was included in the observed intensity as will be described below.

The relative polarized fluorescence intensities as a function of time were computed for each pseudomolecule. Since we considered the trajectories of pseudomolecules, it sufficed to compute only geometrical contributions (at a time t) to the probability ($p[\theta(t), \phi(t)]$) of detecting a polarized photon. The intensities were proportional to the probability of excitation multiplied by $p[\theta(t), \phi(t)]$); so for dipoles uniformly distributed in space:

$$I_{\parallel}(t) \propto \cos^2\theta(0) p_{\parallel}[\theta(t), \phi(t)] \propto \cos^2\theta(0)\,|\hat{\mu}\cdot\hat{k}|^2$$

and

$$I_{\perp}(t) \propto \cos^2\theta(0) p_{\perp}[\theta(t), \phi(t)] \propto \cos^2\theta(0)\,|\hat{\mu}\cdot\hat{j}|^2 \quad (2)$$

or

$$I_{\parallel}(t) \propto \cos^2\theta(0)\ \langle p_{\parallel}[\theta(t)]\rangle \propto \cos^2\theta(0)\cos^2\theta(t)$$

$$I_{\perp}(t) \propto \cos^2\theta(0)\ \langle p_{\perp}[\theta(t)]\rangle \propto 1/2\cos^2\theta(0)\sin^2\theta(t) \quad (3)$$

where eq 2 has been averaged over $\phi(t)$ to account for the time-independent azimuthial symmetry.[2,3]

The trajectories were generated according to the equation of Perrin (1934):

$$\Delta\omega_j = \pm[2D_j(\Delta t)]^{1/2} \qquad j = 1, 2, 3 \qquad (4)$$

where the $\Delta\omega_j$ refer to angles of rotation about the semiaxes of a tumbling ellipsoid of revolution and the D_j are the rotational diffusion constants about these axes (see below). The Δt were chosen long compared to the solvent collison frequency (approximately 10^{-12} s) but small enough so that cos $(\Delta\omega_j) \simeq (1 - \Delta\omega_j)$. The rotary motion was generated by successive Euler transformations about the 1, 2, and 3 axes with the magnitude given by eq 4 and direction (sign) chosen by a random-number generator. If a boundary were exceeded by any rotation, the program was reset to the geometry used prior to that rotation. This reflection was not allowed to take any time as would be required in stochastic calculations involving particle trajectories near boundaries. In the present case the physical reflection was very fast compared to Δt in eq 4 (the time interval during which the average displacement occurs) so that the pseudomolecule kinematics could be ignored. This technique of reflection essentially assumes eq 4 to hold within an inner cone-shaped region located $\Delta\omega_j$ (j = 1, 2) (typically 1.5°) away from the barrier.

The rotary diffusion constants ($D = D_1 = D_2$) for end-over-end motion of the tethered S-1 moiety were determined using a theorem of Yu and Stockmayer (1967). Applied to the present problem, this theorem states that for sufficiently long S-1 moieties of length l:

[2] Harvey and Cheung (1972) have used different expressions in their numerical calculations of fluorescence depolarization (without boundaries). They have acknowledged an error in their equations (equivalent to eq 2 and 3) (S. Harvey, private communication). Several of the cases they considered have been recalculated and very little difference between the present method, their results, and Belford et al.'s (1972) analytical predictions were found.

[3] Equations 2 and 3 may be immediately generalized by associating the absorption dipole with the $\cos^2\theta(0)$ factor and the emission dipole with factors containing $\theta(t)$.

$$D^{\text{attached}}(l) = 2 \times D^{\text{free}}(2l) \quad (5)$$

The application of this theorem to free myosin flexibility has been justified experimentally (Mendelson et al., 1973; main text). The rotary diffusion about the major axis (D_3) was taken as that of an ellipsoid of length $2l$; however, large variations in D_3 did not affect the resulting depolarization.

After a number (usually 48) of Δt intervals (16 complete Euler angle transformations), the intensities were computed according to eq 3 and stored in the computer memory. This process was repeated until the end of the time interval was reached. Repeating the entire process for the N pseudomolecules and number averaging yield the polarization anisotropy (eq 1).

Results of the Calculations. The program to compute the depolarization was implemented on the University of California Lawrence Berkeley Laboratory CDC 7600. The systems random-number generator "RANF" was used. The following results required a total of approximately 10^8 rotations.

Figure 7 shows the effect of the barrier on depolarization curves. The curves consist of two parts, a rapidly decaying region and a component which asymptotically approaches a nonzero value. The latter corresponds to real dipoles becoming completely randomized within the cones but retaining some orientation in the laboratory system because of the boundaries.[4]

Due to the short lifetime of the dye and the shape of the lamp pulse, we could only measure the decay reliably in a limited time region. The results of the numerical calculations and of the experiments were fitted by least squares to a single exponential decay over a region between 26 and 113 ns after $t = 0$. The calculated rotational correlation time (ϕ) of this exponential is plotted in terms of its percent change from the analytical (no boundary) value vs. the half angle of the cone (δ_{max}) in Figure 8.

The significant feature of these curves is their dramatic increase below $\delta_{max} = 20°$. Thus, if a large increase in ϕ is observed experimentally, as it is in myosin thick filaments, considerable immobilization has occurred. This has been exploited in the study of the possible effect of Ca^{2+} on moving the crossbridge radially away from the thick filaments (Mendelson & Cheung, 1976) and for setting a limit on crossbridge mobility in thick filaments (see main text).

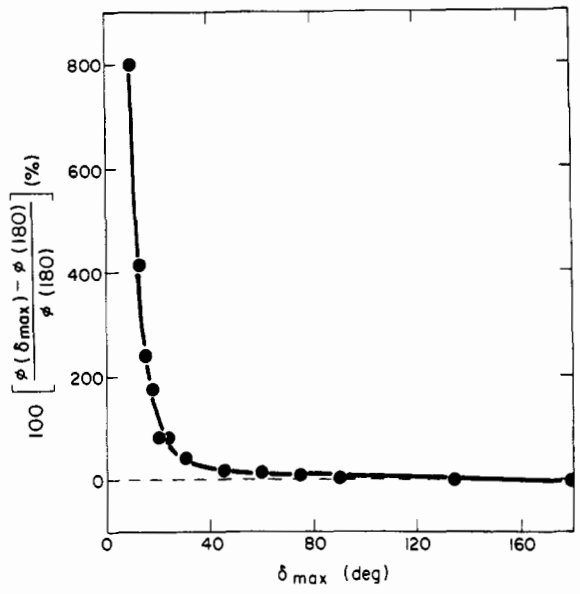

FIGURE 8: The percent change in ϕ from the unconstrained case vs. the half angle (δ_{max}) of the cone. Conditions were the same as in Figure 7, except that 2×10^3 pseudomolecules were used in computing each point.

Note Added in Proof

The theory of fluorescence depolarization within cone-shaped boundaries was generalized to consider absorption and emission dipoles in arbitrary orientations. The symmetry axes of the pseudomolecules and of the cones filled space uniformly at $t = 0$. Each $\cos^2[\theta_{abs}(0)]$ was determined by transforming the orientation of the absorption dipole from the pseudomolecule (body fixed) coordinates to the laboratory reference frame. After rotations [using eq 5 and $D_3(l)$], $\theta_{em}(t)$ was determined in the same manner and the intensities were computed using the modification of eq 3 discussed in footnote 3. The polar angles in the body-fixed system were defined θ_α and θ_ϵ for absorption and emission dipoles, respectively. Calculations were performed for a dipole separation of 25° with dipoles with the following body-fixed polar angle pairs (θ_α, θ_ϵ): (0°, 25°), (12.5°, 12.5°), (20°, 20°), (20°, 35°). Single exponential least-squares fits to the constrained and unconstrained cases were performed between 26 and 113 ns. No significant differences from points in Figure 8 (0°, 0°) could be found, thus verifying conclusions drawn from this simpler case.

[4] Note that $\lim_{t \to \infty} r(t)/r(0)$ is a function which depends only on the geometry of the boundary and thus may be readily computed. In practice it may be difficult to measure if the diffusion times are long relative to the dye lifetime.

References

Bagshaw, C. (1977), *Biochemistry 16,* 59.
Belford, G. F., Belford, R. L., and Weber, G. (1972), *Proc. Natl. Acad. Sci. U.S.A. 69,* 1392.
Biro, N. A., Szilagyi, L., and Balint, M. (1972), *Cold Spring Harbor Symp. Quant. Biol. 37,* 55.
Curtin, N. A., Gilbert, C., Kretzschmar, K. M., and Wilkie, D. R. (1974), *J. Physiol. (London) 238,* 455.
Harvey, S. C., and Cheung, H. C. (1972), *Proc. Natl. Acad. Sci. U.S.A. 69,* 3670.
Haselgrove, J. (1975), *J. Mol. Biol. 92,* 113.
Highsmith, S. (1977), *Biophys. J. 17,* 40a.
Huxley, A. F., and Simmons, R. M. (1971), *Nature (London) 233,* 533.
Huxley, H. E. (1969), *Science 164,* 1356.
Huxley, H. E., and Brown, W. (1967), *J. Mol. Biol. 30,* 383.
Kaminer, B., and Bell, A. L. (1966), *J. Mol. Biol. 20,* 391.
Lowey, S., and Margossian, S. S. (1974), *J. Mechanochem. Cell Motil. 2,* 241.
Lowey, S., Slayter, H. S., Weeds, A. G., and Baker, H. (1969), *J. Mol. Biol. 43,* 1.
Margossian, S. S., and Lowey, S. (1973a), *J. Mol. Biol. 74,* 301.
Margossian, S. S., and Lowey, S. (1973b), *J. Mol. Biol. 74,* 313.
Margossian, S. S., and Lowey, S. (1976), *Fed. Proc., Fed. Am. Soc. Exp. Biol. 35,* 1580.
Margossian, S. S., and Lowey, S. (1977), *Biophys. J. 17,* 37a.
Margossian, S. S., Lowey, S., and Barshop, B. (1975), *Nature (London) 258,* 163.
Mendelson, R. A., and Cheung, P. (1976), *Science 194,* 190.
Mendelson, R. A., Morales, M. F., and Botts, J. B. (1973),

Biochemistry 12, 2250.
Mendelson, R. A., Putman, S., and Morales, M. F. (1975), *J. Supramol. Struct. 3,* 162.
Miller, A., and Tregear, R. T. (1972), *J. Mol. Biol. 70,* 85.
Moore, P. B., Huxley, H. E., and DeRosier, D. (1970), *J. Mol. Biol. 50,* 279.
Morimoto, K., and Harrington, W. F. (1974), *J. Mol. Biol. 88,* 693.
Nihei, T., Mendelson, R. A., and Botts, J. B. (1974), *Proc. Natl. Acad. Sci. U.S.A. 71,* 274.
Perrin, F. (1934), *J. Phys. Radium 10,* 497.
Reedy, M. K., Holmes, K. C., and Tregear, R. T. (1965), *Nature (London) 207,* 1276.
Schreiner, K. E. (1973), *J. Theor. Biol. 40,* 591.
Sutoh, K., and Harrington, W. (1977), *Biochemistry 16,* 2441.
Szent-Györgyi, A. G., Cohen, C., and Phillpott, D. E. (1960), *J. Mol. Biol. 2,* 133.
Takashi, R., Duke, J., Ue, K., and Morales, M. F. (1976), *Arch. Biochem. Biophys. 175,* 279.
Thomas, D. D., Seidel, J. C., Hyde, J. S., and Gergely, J. (1975a), *Proc. Natl. Acad. Sci. U.S.A. 72,* 1729.
Thomas, D. D., Seidel, J. C., and Gergely, J. (1975b) *J. Supramol. Struct. 3,* 376.
Tokiwa, T., and Morales, M. F. (1971), *Biochemistry 10,* 1722.
Tonomura, Y., Appel, P., and Morales, M. F. (1966), *Biochemistry 5,* 515.
Weeds, A. G., and Lowey, S. (1971), *J. Mol. Biol. 61,* 701.
Yguerabide, J. (1972), *Methods Enzymol. 26,* 498.
Yu, H., and Stockmayer, W. (1967), *J. Chem. Phys. 47,* 1369.

Analysis of the Effect of Three Different Allosteric Ligands on Oxygen Binding by Hemocyanin of the Shrimp, *Penaeus setiferus*†

Marius Brouwer,*,‡ Celia Bonaventura, and Joseph Bonaventura§

ABSTRACT: The hemocyanin of the shrimp *Penaeus setiferus* is present in the hemolymph as a high molecular weight aggregate with a sedimentation coefficient of 16 S. This value is characteristic for hexameric arthropodan hemocyanins. Only one band, corresponding to the 16S component, is observed on regular disc gel electrophoresis. Sodium dodecyl sulfate gel electrophoresis shows that the hexamer contains two molecular weight species in a ratio of 1 to 2.6, with estimated molecular weights of 82 000 and 77 000, respectively. The 16S aggregate is extremely stable. Complete dissociation into its constituent polypeptide chains can only be achieved under conditions where the protein loses its oxygen binding capacity. The oxygen binding properties of *Penaeus* hemocyanin have been studied. Analytical ultracentrifugation verified that the sedimentation coefficient of the oxy- and deoxyhemocyanin was 16 S in all of the conditions used in the binding studies. The oxygen affinity of *Penaeus* hemocyanin can be modulated by three different allosteric effectors: hydrogen ions, calcium ions, and chloride ions. Hydrogen ions decrease the oxygen affinity of *Penaeus* hemocyanin. There is a very strong positive Bohr effect. Calcium and chloride ions increase the oxygen affinity of *Penaeus* hemocyanin, opposing the effect of hydrogen ions. The possible physiological significance of these effects is discussed. The oxygen binding data could not be described by the allosteric two state model of J. Monod et al. ((1965) *J. Mol. Biol. 12,* 88–118). The introduction of one symmetrical hybrid state, R_3T_3, resulted in an excellent fit between theory and experiments.

Hemocyanins have been studied extensively, as elaborate models of cooperative and allosteric interactions, over the past few years. Information about the oxygen binding properties of these high molecular weight proteins is rapidly increasing (Van Holde & van Bruggen, 1971; Bonaventura et al., 1977). Hemocyanins fall into two classes, molluscan and arthropodan hemocyanins, both of which bind 1 O_2 per 2 copper atoms. The molluscan hemocyanins have a functional unit with a minimum molecular weight of 50 000. Their subunits contain multiple oxygen binding domains and the multisubunit aggregate may contain as many as 180 binding sites. Arthropodan hemocyanins have 75 000–80 000 dalton subunits. In arthropodan hemocyanins the multisubunit aggregate commonly contains 6, 12, 24, or 48 oxygen binding sites (Van Holde & van Bruggen, 1971; Bonaventura et al., 1977). One of the interesting problems in studying the oxygen binding by these multisubunit proteins concerns the question of how many sites are involved in the cooperative interactions. Do these interactions involve all the binding sites, or are they confined to subgroups or functional constellations each containing a fixed number of strongly interacting sites, responsible for most of the cooperativity shown by the entire system. Do secondary interactions exist between these functional constellations? The answer to these questions seems to depend upon the class of hemocyanins under study.

Molluscan hemocyanins can be easily dissociated into 1/10 molecules which have about 18 binding sites. The 1/10 molecules of *Helix pomatia* α-hemocyanin at pH 8.2, ionic strength 0.1, have oxygen binding properties corresponding to those of the high affinity state of the undissociated molecules at pH 8.2 in the presence of 10 mM $CaCl_2$. However, when these 1/10 molecules are surrounded in the whole molecule by 1/10 molecules whose oxygen binding sites have been made inactive

† From Duke University Marine Laboratory, Beaufort, North Carolina 28516. *Received December 16, 1977.* This work was supported by grants from the National Science Foundation (BMS 75-15246) and the National Institutes of Health (HL 15460).
‡ Supported by the Netherlands Organization for the Advancement of Pure Research.
§ Established Investigator of the American Heart Association.

0006-2960/78/0417-2148$01.00/0